Evaluating Hydrogen Evolution and Oxidation in Alkaline Media to Establish Baselines

Shaun M. Alia *,z **and Bryan S. Pivovar***

Chemistry and Nanoscience Center, National Renewable Energy Laboratory, Golden, Colorado 80401, USA

This paper fills a significant gap in the literature for alkaline hydrogen evolution (HER) and oxidation (HOR) baseline performance, while reviewing the different variables that influence observed properties. Although high-performing HER-HOR catalysts in acidic electrolytes are too active to measure kinetic in rotating disk electrode (RDE) half-cells, under alkaline conditions RDE kinetics evaluations are relevant and half-cell performances are comparable to hydrogen pump data. This paper focuses on best practices to ensure that half-cell tests don't unnecessarily lower platinum group metal (PGM) performance or improve non-PGM performance. Specific aspects examined include experiments on PGMs minimizing the impact of impurities (electrolyte, cell material) and experiments on non-PGMs minimizing the impact from test protocols (counter electrode).
 [DOI: 10.1149/2.0361807jes]

Manuscript submitted January 22, 2018; revised manuscript received March 26, 2018. Published April 28, 2018. This was Paper 1662 presented at the National Harbor, Maryland Meeting of the Society, October 1–5, 2017.

Alkaline hydrogen evolution (HER) is a growing area of interest, largely driven by the possibility of performing electrolysis with non-platinum (Pt) group metal (PGM) catalysts in alkaline media. Although numerous efforts have focused on improving HER and hydrogen oxidation (HOR) activity[1–7] and developing PGM[8–10] and non-PGM catalysts,[11–23] a comprehensive baselining paper doesn't exist. This has led to a number of difficulties for the community that are highlighted in this paper, including using robust PGM performance and durability baselines and using test protocols that don't artificially lessen the gap between PGMs and non-PGMs. We have pursued establishing alkaline HER-HOR baselines to fill this gap and since it is necessary for the community to build on.

Studies attempting to obtain rotating disk electrode (RDE) kinetic data in acid are usually fruitless because the kinetic rates of high performing catalysts are so high that mass transport becomes the limiting factor.[24,25] This has resulted in a lack of agreement, where RDE half-cell performance is significantly lower than membrane electrode assemblies (MEAs) in hydrogen pump data.[24] RDE measurements are relevant in alkaline media where kinetic rates are slower and therefore can be separated from mass transport.[25] Under alkaline conditions, half-cell performances (exchange current densities) are comparable to MEA-hydrogen pump data and RDE-HOR does not meet the Nerstian diffusion limited overpotential in the kinetic region.[25,26]

This paper focuses on protocols and best practices to ensure that half-cell tests don't unnecessarily lower PGM performance or improve non-PGM performance, and includes: PGM experiments on minimizing the impact of impurities (electrolyte, cell material); and non-PGM experiments on minimizing the impact from test protocols (counter electrode). Electrochemical baselines for alkaline HER-HOR performance have previously been investigated, and the specific test concerns evaluated here have been studied to some extent elsewhere.[3,4,6–8,25,27–29] Mayrhofer and Arenz et al. among others have demonstrated the impact of glass corrosion and related contaminants on performance evaluations; this study, however, adheres to more typical testing conditions (cycling > 0.5 V) to evaluate the necessity of polytetrafluoroethylene cells under standard test protocols.[28,30] Markovic et al. among others have examined electrolyte impurities, demonstrating an effect on Pt; this work, however, evaluates a variety of commercially available electrolytes in an effort to minimize contaminant contributions on testing.[31] Additionally, Pt dissolution concerns at elevated potential are obvious and addressed in a variety of publications; this work, however, uses electrochemical conditioning procedures adapted from literature to quantify how test choices can overestimate non-PGM HER kinetics. This work is focused on bringing these different aspects together under standardized testing parameters, to set realistic expectations for the kinetic capabilities of various materials in HER-HOR.

These baseline studies were pursued for the community to build on in alkaline HER catalyst development for electrolysis applications. Electrolysis, or electrochemical water splitting, is currently used in limited commercial applications, but greater use is expected for hydrogen consuming applications (transportation, agriculture) and energy storage with increasing use of low-cost renewables.[32–35] Anion exchange membrane (AEM)-based electrolyzers are attractive because non-PGM catalysts can potentially provide high performance and improved durability.[1,2,36,37] In alkaline media oxygen evolution is kinetically slower than HER (~3 orders of magnitude in AEM); slower HER kinetics (compared to acid) means that catalyst performance/loading is a crucial consideration.

Experimental

Polished metal electrodes were evaluated and included Pt (Pine Research Instrumentation, AFE5T050PT), palladium (Pd, Pine Research Instrumentation, AFE5T050PD), and nickel (Ni, American Elements, NI-M-03M-D.4MMT). Nanoscale catalysts were evaluated and included Pt nanoparticles supported on high surface area carbon (Pt/HSC, Tanaka Kikinzoku Kogyo, TEC10E50E), Pt nanoparticles supported on Vulcan (Pt/Vu, Tanaka Kikinzoku Kogyo, TEC10V50E), Pt-ruthenium (Ru) nanoparticles supported on Vulcan (PtRu/Vu, Alfa Aesar, 44172), Pd nanoparticles supported on Vulcan (Pd/Vu, Alfa Aesar, A12012), and Ni nanoparticles (Alfa Aesar, 45505). These materials were chosen because: Pt is a commonly used HER-HOR catalyst; Pt-Ru provides nominal improvement to Pt; Pd is a commonly used PGM alternative to Pt; and Ni is the most commonly investigated non-PGM HER catalyst.

Nanoscale catalyst surveys were completed at loadings of 17.8 μg_M $cm_{elec}{}^{-2}$. Inks contained 3.49 mg of metal in 7.6 ml water and 2.4 ml isopropanol. The metal mass corresponded to 7.60 mg Pt/HSC (45.9 wt% Pt), 7.52 mg Pt/Vu (46.4 wt% Pt), 5.81 mg PtRu/Vu (60 wt% Pt-Ru), 34.89 mg Pd/Vu (10 wt% Pd), and 3.49 mg Ni (unsupported). The inks were iced for 5 min, and Nafion ionomer (5 wt%, Sigma Aldrich, 527084) was added to an ionomer to carbon ratio (I:C) of 0.45. Since the Ni nanoparticles were unsupported, the ionomer content was kept constant to Pt/HSC on a metals basis (I:metal 0.38). After 20 min of bath sonication in ice, 10 µl of ink were pipetted onto glassy carbon electrodes (Pine Research Instrumentation, AFE5T050GC) rotating at 100 rpm. The electrodes were dried for 20 min in air at room temperature, after the rotation was increased to 700 rpm.

*Electrochemical Society Member.
zE-mail: shaun.alia@nrel.gov

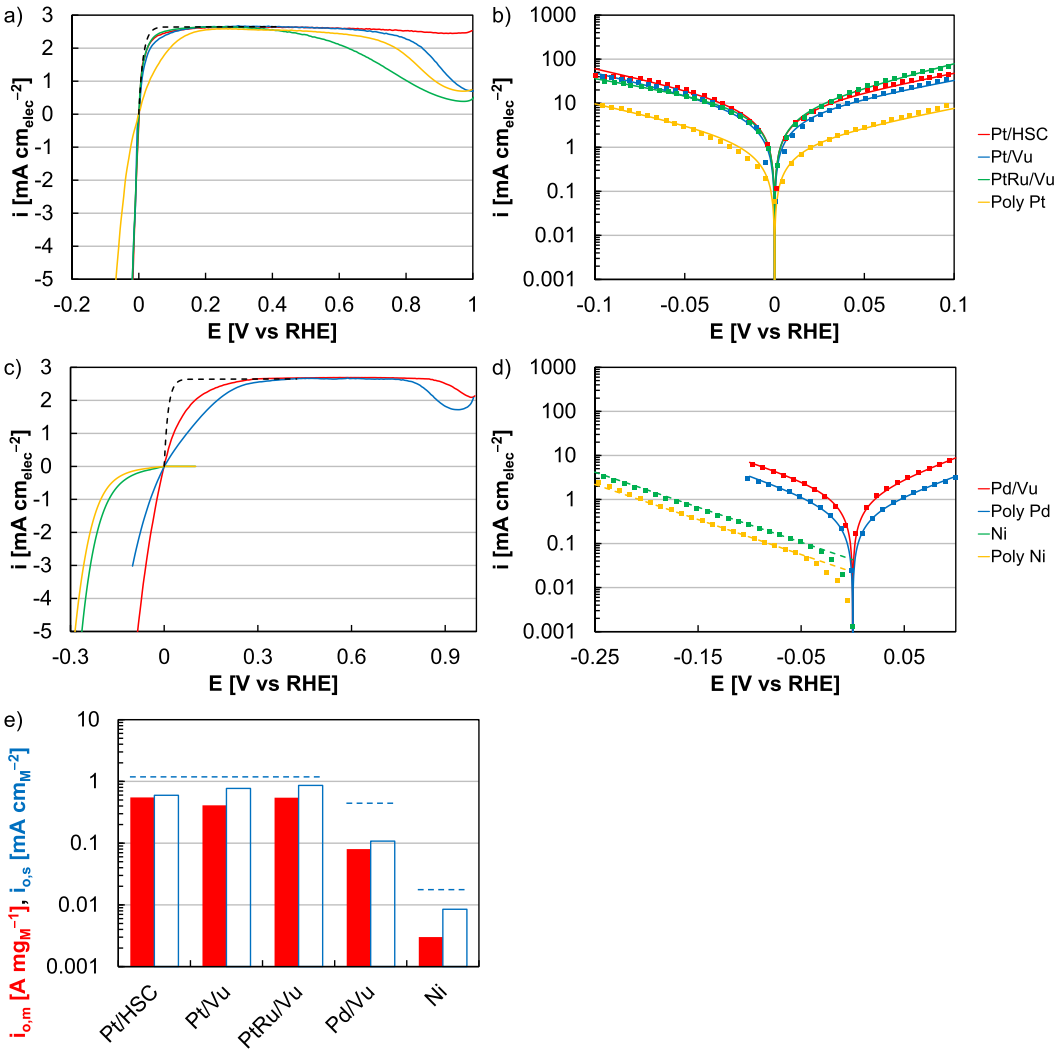

Figure 1. (a) Polarization curves and (b) Butler-Volmer fits of Pt/HSC, Pt/Vu, PtRu/Vu, and a polished Pt electrode (Poly Pt). (c) Polarization curves and (d) Butler-Volmer/Tafel fits of Pd/Vu, a polished Pd electrode (Poly Pd), unsupported Ni (Ni), and a polished Ni electrode (Poly Ni). Polarization curves were taken cathodically at 10 mV s^{-1} and 2500 rpm using a 0.1 M NaOH electrolyte (Honeywell Research Chemicals, TraceSELECT) in polytetrafluoroethylene cells. The dashed black line (a, c) is the Nernstian diffusion limited overpotential. (e) Summary of mass (red) and specific (blue) exchange current densities, with dashed blue lines corresponding to the specific activities of metal electrodes (Pt, Pd, Ni, lines above respective commercial nanoparticles).

Studies were performed to evaluate the effect of ionomer content and catalyst loading on performance. Ionomer contents of 0, 0.1, 0.45, and 0.8 were tested, and the inks were identical to those described above with the exception of the amount of ionomer added. Pt/HSC loadings of 4.5, 8.9, 17.8, 35.6, and 71.2 μg cm_{elec}^{-2} were tested, and the inks were adjusted by modifying the catalyst concentration while keeping the ionomer content (I:C ratio 0.45) constant.

Nafion ionomer was used in inks for the testing of nanoparticle-based catalysts (Pt, Pt-Ru, Pd, Ni). Nafion ionomer would not be used in AEM-based MEAs, since the ionomer is needed to transport hydroxide between the catalyst site and membrane. Since the half-cell tests were conducted in a liquid alkaline electrolyte, a hydroxide conductor was not needed. Nafion ionomer was added in small amounts to improve ink dispersion and catalyst performance, and some optimization was completed for all catalysts evaluated. The Nafion ionomer was provided in proton form and was not converted prior to its use in catalyst inks or electrochemical testing. Although in the proton form, the Nafion ionomer was not acidic as soon as it contacted the alkaline electrolyte. Ionomer use also did not result in catalyst dissolution (Pt, Pt-Ru, Pd, Ni), confirmed in inductively coupled plasma mass-spectrometry (ICP-MS) for all electrolytes regardless of test parameters (conditioning, durability testing) and the amount of Nafion ionomer added. In all cases, dissolved metal amounts were comparable to the detection limit of the ICP-MS (approximately 1 ppt Pt, Ru, Pd and 10 ppt Ni) and represented less than 0.04 wt% of the catalyst mass on the working electrode.

Catalysts were evaluated in RDE half-cells using a three electrode setup. A modulated speed rotator (Pine Research Instrumentation, AFMSRCE) controlled working electrode rotation and electrochemical measurements were taken with an Autolab PGSTAT302N potentiostat (Eco Chemie, Metrohm Autolab). Pt, gold (Au), or carbon counter electrodes were used depending on the experiment, and different reference electrodes were used depending on whether tests were completed in polytetrafluoroethylene (Pine Research Instrumentation, ALK-R-CELL-1) or glass electrochemical cells. The glass electrochemical cell incorporated a bubbler into the cell body design; for the polytetrafluoroethylene cell, a pipette tip (0.1−1.0 ml) was used. The polytetrafluoroethylene cell used a mercury/mercurous oxide reference electrode (Koslow Scientific Company, 5088) connected to the main cell by a handmade Luggin capillary formed by heating a heat-shrinkable polytetrafluoroethylene sleeve (Koslow Scientific Company, 5089). The glass cell used a Pt wire in a hydrogen-saturated electrolyte connected to the main cell by a Luggin capillary as a reversible hydrogen electrode (RHE) reference. Although later portions

Table I. Survey of published mass ($i_{0,m}$) and specific ($i_{0,s}$) exchange current densities of nanoparticle-based Pt (Nano Pt), Pt-Ru (Nano Pt-Ru), Pd (Nano Pd), and Ni (Nano Ni) baseline catalysts, along with the published specific exchange current densities of polished Pt, Pd, and Ni electrodes.[a,b]

Author	Ref.	Type	Details	% Metal [wt%]	$i_{0,m}$ [A mg_M^{-1}]	$i_{0,s}$ [mA cm_M^{-2}]
Platinum nanoparticles						
This work		Nano Pt	TKK	46	0.550	0.595
Gasteiger et al.	6	Nano Pt	TKK	5	1.2	1
Abruña et al.	46	Nano Pt	Not specified	–	0.393	0.48
Wang et al.	47	Nano Pt	TKK	46	0.38	–
Gasteiger and Shao-Horn et al.	25	Nano Pt	TKK	46	0.35	0.57
Yan et al.	10	Nano Pt	Not specified	–	0.35	0.58
Yan et al.	48	Nano Pt	Not specified	–	0.35	0.58
Papandrew et al.	8	Nano Pt	Self-made	–	0.265	0.49
Xu and Yan et al.	49	Nano Pt	Premetek	5	–	0.48
Yan and Chen et al.	50	Nano Pt	TKK	46	–	0.479
Jiang, Fu, Xie et al.	51	Nano Pt	Alfa Aesar	20	–	0.458
Wong et al.	52	Nano Pt	Not specified	–	–	0.202
Ohyama and Satsuma et al.	53	Nano Pt	Not specified	–	0.18	0.195
Markovic et al.	54	Nano Pt	TKK	–	0.145[c]	–
Gong et al.	55	Nano Pt	Not specified	–	0.166[c]	–
Mukerjee et al.	56	Nano Pt	TKK	46	0.0726	–
Tang et al.	57	Nano Pt	JM	20	–	0.0676[c]
Ohyama et al.	58	Nano Pt	TKK	50	0.0676[c]	0.0573[c]
Mukerjee et al.	59	Nano Pt	Not specified	–	0.067[c]	–
Mukerjee et al.	60	Nano Pt	TKK	47	0.0408[c]	–
Serov et al.	61	Nano Pt	Not specified	–	0.0121[c]	–
Xu et al.	62	Nano Pt	Not specified	20	0.00292	–
Jing and Yin et al.	63	Nano Pt	Not specified	–	0.00283[c]	–
Qiao et al.	64	Nano Pt	Not specified	–	0.001813	0.002342
Asefa et al.	65	Nano Pt	Sigma Aldrich	1	2.16E-07[c]	–
Polished Pt						
This work		Pt		–	–	1.21
Markovic et al.	66	Pt		–	–	1[c]
Yan et al.	10	Pt		–	–	0.75
Yan and Chen et al.	50	Pt		–	–	0.741
Markovic et al.	67	Pt		–	–	0.728
Gasteiger et al.	68	Pt		–	–	0.7
Gasteiger and Shao-Horn et al.	25	Pt		–	–	0.69
Yan et al.	3	Pt		–	–	0.631
Chen and Yan et al.	13	Pt		–	–	0.61
Gasteiger et al.	38	Pt		–	–	0.55
Chen and Yan et al.	69	Pt		–	–	0.53
Markovic et al.	70	Pt		–	–	0.441[c]
Santos et al.	71	Pt		–	–	0.00103
Pt-Ru Nanoparticles						
This work		Nano Pt-Ru	Alfa Aesar	60	0.545	0.861
Mukerjee et al.	56	Nano Pt-Ru	JM	20	0.988[c]	–
Papandrew et al.	8	Nano Pt-Ru	Self-made	–	0.696	1.42
Ohyama and Satsuma et al.	53	Nano Pt-Ru	Not specified	–	0.39	0.585
Papandrew et al.	8	Nano Pt-Ru	Self-made	–	0.345	0.41
Wang et al.	47	Nano Pt-Ru	TKK	53	0.3096	–
Mukerjee et al.	60	Nano Pt-Ru	ETEK	58	0.105[c]	–
Serov et al.	61	Nano Pt-Ru	Not specified	–	0.0114[c]	–
Pd Nanoparticles						
This work		Nano Pd	Alfa Aesar	10	0.0800	0.108
Gasteiger et al.	6	Nano Pd	Premetek	10	0.063	0.06
Yan et al.	48	Nano Pd	Not specified	–	0.04	0.05
Yan et al.	72	Nano Pd	Premetek	20	0.038	0.052
Xu and Yan et al.	49	Nano Pd	Premetek	20	–	0.045
Abruña et al.	46	Nano Pd	Not specified	–	0.0333	0.025
Papandrew et al.	8	Nano Pd	Self-made	–	0.02215	0.05
Polished Pd						
This work		Pd		–	–	0.501
Yan et al.	48	Pd		–	–	0.18
Yan et al.	3	Pd		–	–	0.126
Ni Nanoparticles						
This work		Nano Ni	Alfa Aesar	100	0.00301	0.00848
Xu et al.	62	Nano Ni	Self-made	100	0.0000356	–

Table I. (Continued).

Author	Ref.	Type	Details	% Metal [wt%]	$i_{0,m}$ [A mg_M^{-1}]	$i_{0,s}$ [mA cm_M^{-2}]
Polished Ni						
This work		Ni		–	–	0.0199
Shervedani et al.	73	Ni		–	–	0.02
Markovic et al.	67	Ni		–	–	0.018[c]
Tanaka et al.	74	Ni		–	–	0.0109
Weininger and Breiter	75	Ni		–	–	0.01
Ângelo et al.	76	Ni		–	–	0.009
Yan et al.	3	Ni		–	–	0.00794
He et al.	77	Ni		–	–	0.007
Oshchepkov et al.	78	Ni		–	–	0.0022
Shervedani et al.	79	Ni		–	–	0.002
Kubisztal et al.	80	Ni		–	–	0.00108
Li et al.	81	Ni		–	–	0.00112
Pérez-Herranz et al.	82	Ni		–	–	0.00016
Kellenberger et al.	83	Ni		–	–	0.0000257

[a]Values were only included for experiments conducted on HER-HOR (not photo-assisted or combined processes) in alkaline electrolytes (not acidic or buffers) and focused on baseline materials. References to catalyst development efforts that tuned composition or structure to improve material performance were generally avoided; self-made materials that focused on reaction mechanisms, however, were included.
[b]Values were not included for publications that referenced baselines from other publications. The values of the original (referenced) publication were included provided that the experiment was conducted in an alkaline electrolyte.
[c]Exchange current densities were approximated for publications that provided polarization curves but did not calculate exchange current densities. For Pt, Pt-Ru, and Pd catalysts, the exchange current densities were approximated by the Butler-Volmer equation assuming an anodic charge transfer coefficient of 0.5 and fit to the HER portion, since HOR approximations were difficult in the limited potential range between 0 V and the diffusion limited current. For Ni, the exchange current density was approximated using the Tafel equation and fit to the HER portion using two data points (to approximate a Tafel slope). Values were not provided for publications that did provide an experimental RHE correction.

of this paper investigate the impact of a Pt counter electrode on performance evaluations, a Pt-based reference electrode was of less concern because: the reference sees lower potential (0 V) than the counter ($\geq$ 2.5 V); and Ni evaluations used the polytetrafluoroethylene cell with a mercury/mercurous oxide reference electrode.

Electrochemical cells were cleaned by submerging in a sulfuric acid bath overnight, followed by a Nochromix bath overnight. The cells were then boiled in 18 MΩ deionized water eight times prior to testing, and were stored in 18 MΩ deionized water when not in use.

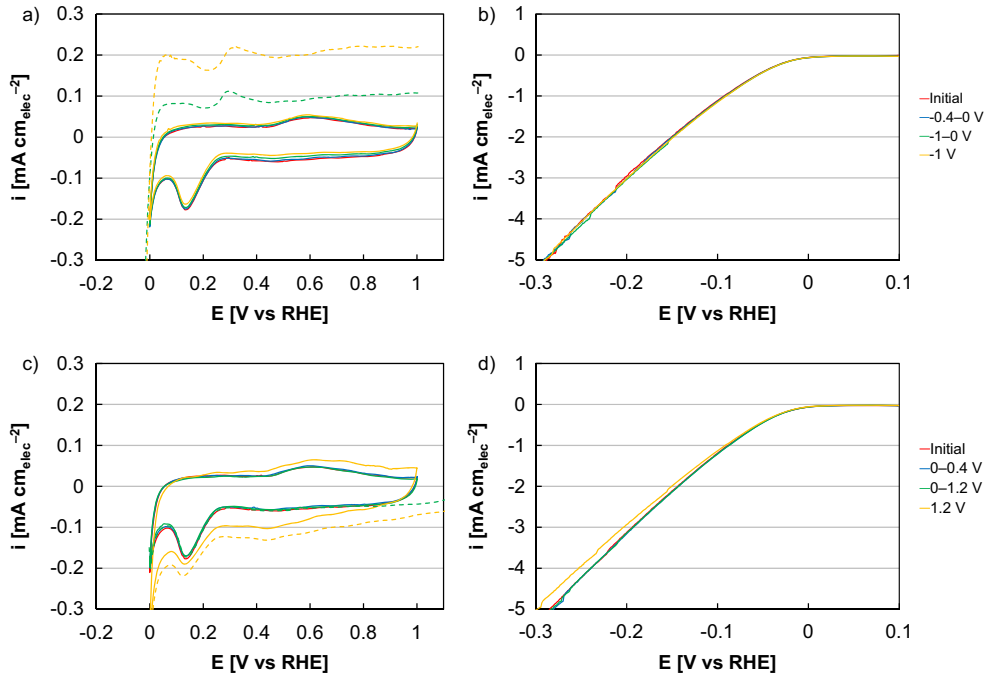

Figure 2. (a) Cyclic voltammograms and (b) polarization curves of Ni nanoparticles following conditioning at negative potential, including: red, first scan with no conditioning; blue, 10 cycles −0.4–0 V vs. RHE; green, 10 cycles −1–0 V vs. RHE; and yellow, 10 min hold at −1 V vs. RHE. (c) Cyclic voltammograms and (d) polarization curves of Ni nanoparticles following conditioning at positive potential, including: red, first scan with no conditioning; blue, 10 cycles 0–0.4 V vs. RHE; green, 10 cycles 0–1.2 V vs. RHE; and yellow, 10 min hold at 1.2 V vs. RHE. Cyclic voltammograms were taken at 20 mV s^{-1} and polarization curves were taken cathodically at 10 mV s^{-1} and 2500 rpm using a 0.1 M NaOH electrolyte (TraceSELECT, Honeywell Research Chemicals).

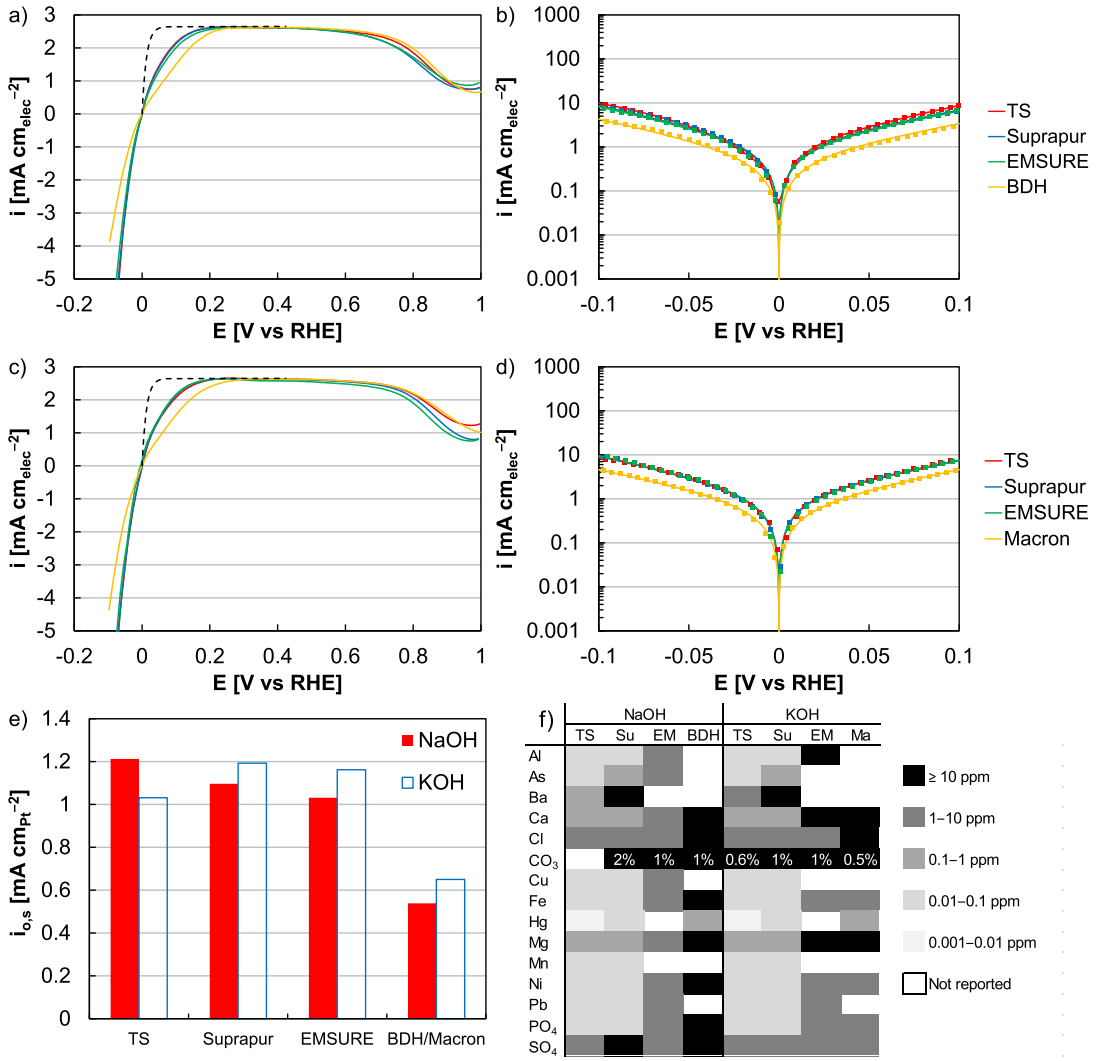

Figure 3. (a, c) Polarization curves and (b, d) Butler-Volmer fits of a polished Pt electrode using 0.1 M (a−b) NaOH and (c−d) KOH electrolytes. Polarization curves were taken cathodically at 10 mV s^{-1} and 2500 rpm in polytetrafluoroethylene cells. The dashed black line (a, c) is the Nernstian diffusion limited overpotential. (e) Summary of specific exchange current densities for NaOH (red) and KOH (blue). Tested electrolytes include TraceSELECT (TS, Honeywell Research Chemicals), Suprapur (Su, EMD Millipore), EMSURE (EM, EMD Millipore), BDH (sodium hydroxide, VWR International), and Macron (Ma, potassium hydroxide, Avantor Performance Materials). (f) Table of tested sodium and potassium hydroxide electrolytes with selected contaminants, color coded (darker corresponding to increased concentration) based on binning: 0.001−0.01 ppm; 0.01−0.1 ppm; 0.1−1 ppm; 1−10 ppm; and ≥ 10 ppm. The sodium or potassium carbonate (CO_3) content was also listed by percentage.

For Pt/HSC, Pt/Vu, and Pd/Vu, electrodes were electrochemically conditioned in 0.1 M perchloric acid (50 cycles, 0.025−1.0 V vs RHE) in a separate glass electrochemical cell prior to being rinsed in water and tested in alkaline electrolytes. This process improved electrochemical surface area (ECA) and HER-HOR performance. This process was not completed on PtRu/Vu or Ni, since it resulted in excessive dissolution (Ru, Ni) and lower measured activity.

A number of sodium and potassium hydroxide sources were evaluated. For sodium hydroxide, these sources included TraceSELECT (Honeywell Research Chemicals, 01968, formerly Sigma Aldrich), Suprapur (EMD Millipore, 106466), EMSURE (EMD Millipore, 106495), and BDH (VWR International, BDH9292). For potassium hydroxide, these sources included TraceSELECT (Honeywell Research Chemicals, 60371, formerly Sigma Aldrich), Suprapur (EMD Millipore, 105002), EMSURE (EMD Millipore, 105021), and Macron (Avantor Performance Materials, 6984). Outside of the electrolyte survey, TraceSELECT sodium hydroxide (Honeywell Research Chemicals) was used throughout the study, since it produced HER-HOR activity on a polished Pt electrode representative of higher purity electrolytes. For this electrolyte source, 0.01, 0.1, and 1.0 M were evaluated; a 0.1 M concentration was used throughout the remainder of the study since it resulted in optimal performance on a polished Pt electrode.

Electrochemical conditioning in alkaline electrolytes was completed for 20 cycles at 2500 rpm and 500 mV s^{-1} in an electrolyte bubbled with hydrogen; the potential range, however, depended on catalyst type. PGM catalysts (Pt, Pt-Ru, Pd) were cycled −0.1−1.0 V vs RHE. In the case of Pd, particular care was taken to avoid exposing the electrode to less than −0.1 V and formation of Pd hydride. Ni, however, was cycled at lower potential (−0.4−0.0 V vs RHE) to minimize the impacts of oxide layers. Polarization curves (2500 rpm, 10 mV s^{-1}) were completed cathodically in the potential ranges −0.1−1.0 V (Pt, Pt-Ru, Pd) and −0.3−0.1 V (Ni), immediately following conditioning. Testing protocols were set with exposure times in mind (glass dissolution, carbonation), and cycling was typically started prior to complete hydrogen saturation. From bottle to evaluation, it took 10−12 min to prepare (weigh, dissolve), condition (deaerate, cycle), and take polarization curves.

HER-HOR polarization curves were corrected for internal resistance (20−27 Ω, depending on the electrode) and correction values

Table II. Survey of published specific ($i_{0,s}$) exchange current densities of polished Pt electrodes and the electrolytes (type, manufacturer, product) they were tested in.

Author	Ref.	Type	Manufacturer	Product	$i_{0,s}$ [mA cm_M^{-2}]
This work		0.1 M NaOH	Honeywell Research Chemicals	TraceSELECT	1.21
This work		0.1 M NaOH	EMD Millipore	Suprapur	1.10
This work		0.1 M NaOH	EMD Millipore	EMSURE	1.03
This work		0.1 M NaOH	VWR International	BDH	0.538
This work		0.1 M KOH	Honeywell Research Chemicals	TraceSELECT	1.03
This work		0.1 M KOH	EMD Millipore	Suprapur	1.19
This work		0.1 M KOH	EMD Millipore	EMSURE	1.06
This work		0.1 M KOH	Avantor Performance Materials	Macron	0.650
Markovic et al.	66	0.1 M KOH	Sigma Aldrich	Not specified	1
Yan et al.	10	0.1 M KOH	Not specified	Not specified	0.75
Yan and Chen et al.	50	0.1 M KOH	Not specified	Not specified	0.741
Markovic et al.	67	0.1 M KOH	Multipharm, Sigma Aldrich, JT Baker, Alfa Aesar	Not specified	0.728
Gasteiger et al.	68	0.1 M KOH	Merck	Suprapur	0.7
Gasteiger and Shao-Horn et al.	25	0.1 M KOH	Sigma Aldrich	Not specified	0.69
Yan et al.	3	0.1 M KOH	Sigma Aldrich	Not specified	0.631
Chen and Yan et al.	13	0.1 M KOH	Sigma Aldrich	Not specified	0.61
Gasteiger et al.	38	0.1 M NaOH	Sigma Aldrich	TraceSELECT	0.55
Chen and Yan et al.	69	0.1 M KOH	Sigma Aldrich	Not specified	0.53
Markovic et al.	70	0.1 M KOH	Sigma Aldrich	Not specified	0.441
Santos et al.	71	8 M KOH	AnalaR	NORMAPUR	0.00103

were taken with a built in current interrupter at 0.4 V vs RHE. These curves were fit to the Butler-Volmer (Pt, Pt-Ru, Pd) and Tafel (Ni) equations. The observed HOR diffusion limited currents (2.6−2.7 mA cm_{elec}^{-2}) were expected at the elevation (5674 ft) and partial pressure (83.2 kPa) of our labs, and predicted by the Koutecky-Levich equation. Kinetic HER-HOR exchange current densities were corrected for the partial pressure of hydrogen, assuming a 0.6 reaction order.[38] These corrections were completed only for the kinetic comparisons and were not incorporated into either the linear polarization curves or fitting (log plots).

ECA measurements were taken after the activity determinations. Ni ECAs were evaluated by cyclic voltammograms, from the charge due to hydroxide desorption, although similar values could be achieved from capacitance.[39–41] Pt, Pt-Ru, and Pd ECAs were evaluated by carbon monoxide stripping.[42,43] Carbon monoxide experiments were completed by holding a potential of 0.1 V vs RHE for 20 min: 10 min while bubbling carbon monoxide; and the second 10 min while bubbling nitrogen. During the experiment, the working electrode was rotated at 2500 rpm to prevent bubbles from collecting on the surface. The gas flow was adjusted to blanket the electrolyte

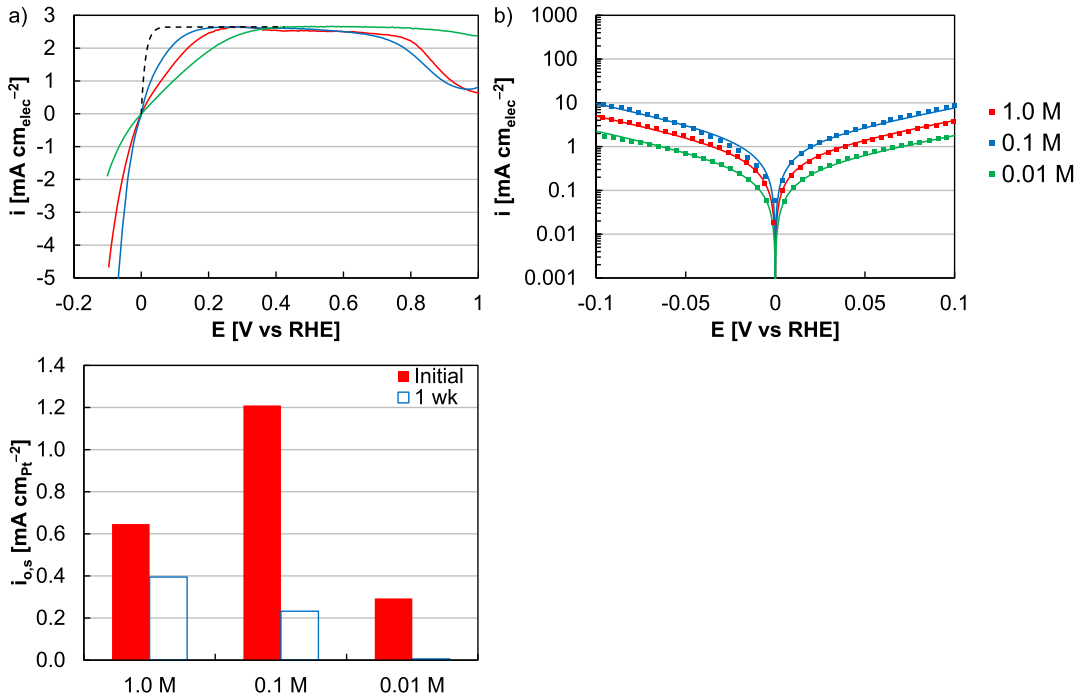

Figure 4. (a) Polarization curves and (b) Butler-Volmer fits of a polished Pt electrode using TraceSELECT NaOH (1.0, 0.1, and 0.01 M) electrolytes. Polarization curves were taken cathodically at 10 mV s^{-1} and 2500 rpm in polytetrafluoroethylene cells. The dashed black line (a) is the Nernstian diffusion limited overpotential. (c) Summary of initial (red) specific exchange current densities and specific exchange current densities in electrolytes that had been aged 1 wk (blue, purged with hydrogen).

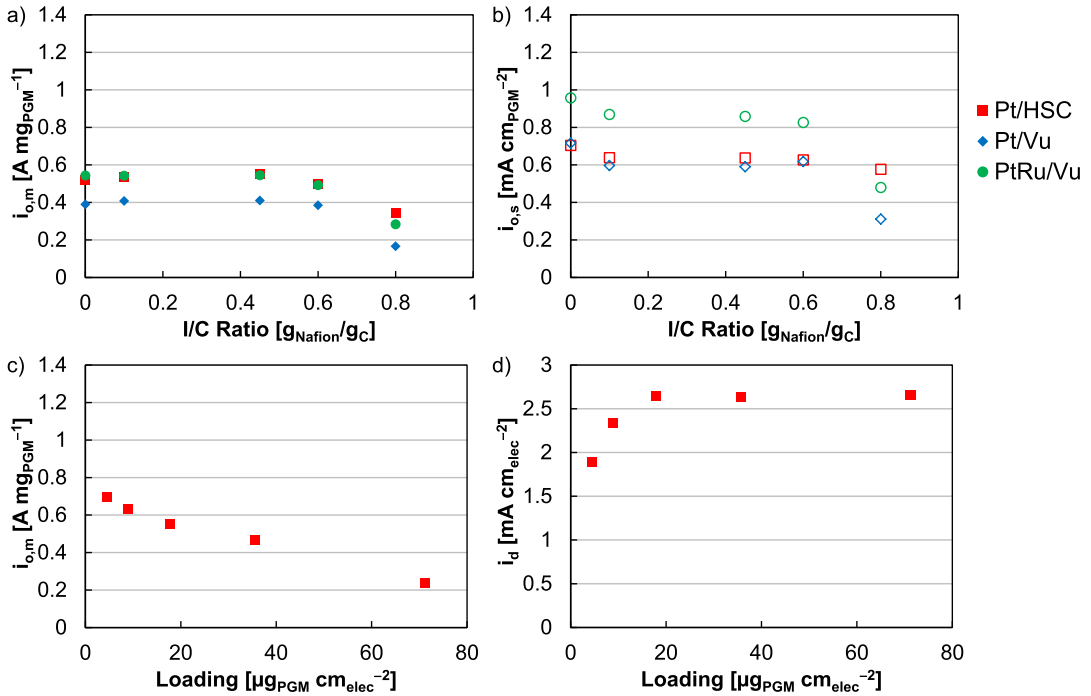

Figure 5. (a) Mass (closed data points) and (b) specific (open data points) exchange current densities of Pt/HSC, Pt/Vu, and PtRu/Vu as a function of the ionomer to carbon ratio (I:C). (c) Mass exchange current densities and (d) diffusion limited currents of Pt/HSC as a function of the electrode loading. Polarization curves were taken cathodically at 10 mV s^{-1} and 2500 rpm in polytetrafluoroethylene cells using a 0.1 M NaOH electrolyte (TraceSELECT, Honeywell Research Chemicals). Inks (c-d) were made with Nafion ionomer at an I:C ratio of 0.45.

and rotation was turned off 30 s prior to the end of the potential hold. Cyclic voltammograms (0.025−1.2 V) were run immediately after, the first cycle for the ECA measurement and subsequent cycles to ensure that carbon monoxide beyond an adsorbed monolayer had not persisted in the electrolyte. Pt and Pt-Ru ECAs were also evaluated by hydrogen underpotential deposition and carbon monoxide stripping in 0.1 M perchloric acid.[43,44] ECA measurements on polished metal electrodes gave roughness factors of 1.21 (Pt), 1.35 (Pd), and 1.63 (Ni) cm_{ECA}^{2} cm_{elec}^{-2}.

Durability tests were completed in polytetrafluoroethylene and glass cells, using Pt, Au, and carbon counter electrodes. Potential cycling was completed in the range −0.2−0.2 V (Pt) and −0.4−0.0 V (Ni) vs RHE, for 100,000 cycles at 2500 rpm and 500 mV s^{-1} in a hydrogen-saturated electrolyte. In the case of electrochemical cell material comparisons (polytetrafluoroethylene vs glass), electrolytes were also aged for 1 wk in a hydrogen-saturated electrolyte without electrode cycling.

Results

The results of this paper have been divided into the subsections Catalyst baselines, Electrochemical cell material, and Counter electrode material, to organize results based on the specific aim of individual experiments. The Catalyst baseline subsection examines the activities of PGM and non-PGM catalysts, commercial nanoparticles and polycrystalline electrodes, as well as investigates the effect of the electrolyte and ink composition on performance. Later subsections examine specific testing concerns, including the choices of: glass versus polytetrafluoroethylene testing cells (Electrochemical cell material); and Pt versus non-Pt counter electrodes and their influence on performance and durability (Counter electrode material).

Catalyst baselines.—Catalyst evaluations were made for commercial nanoparticles and polycrystalline electrodes, for PGM (Pt, Pt-Ru, and Pd) and non-PGM (Ni) catalysts (Figure 1). As previously mentioned, RDE tests in acidic electrolytes are invalid since the experimental setup underestimates Pt kinetics.[24,25] In alkaline electrolytes, however, RDE testing provides useful kinetic data; the validity of this data is confirmed by the similarity between RDE and MEA-hydrogen pump exchange current densities and since the Pt-HOR performance does not meet the Nernstian diffusion limited overpotential in the kinetic region (dashed black line, Figure 1a).[25,26]

Several testing parameters and analysis choices were of importance. HER-HOR activities were evaluated and compared based on their exchange current densities, from the Butler-Volmer equation (HER-HOR) for PGMs and the Tafel equation (HER only) for Ni. Although many non-PGM HER studies make comparisons to Pt based on lost overpotential, exchange current densities were used since these may be better suited for evaluating catalysts' intrinsic capabilities, particularly for reactions (HER-HOR) with fast kinetics, and for ex-situ half-cell tests.[11,14,15,18–21,45] At HER currents greater than 35 mA cm_{elec}^{-2}, transport losses were observed and were not included in the fits (Butler-Volmer) for exchange current density determinations. Polarization curves were also taken in the cathodic direction, since HER on Pt at high current density produced hydrogen bubbles that could reduce the observed HER-HOR current through electrode coverage. Pt and Pd catalysts were generally equally active for HER and HOR (anodic charge transfer coefficients, $\alpha_a = 0.47-0.51$). Pt-Ru, however, was a slight exception and marginally more active for HOR than HER ($\alpha_a = 0.60$). For Ni, no HOR activity was observed, and Ni-HER exchange current densities were evaluated by the Tafel equation.

The performances found in this study were compared to published values in literature, for both nanoparticle-based materials (Pt, Pt-Ru, Pd, Ni) and polished electrodes (Pt, Pd, Ni, Table I). These types of comparisons are complicated by differences in the specific baseline evaluated (manufacturer, composition) and test choices (electrolyte, cell, conditioning, user). They do, however, illustrate the need for universally applied baselines as these performances can vary by several orders of magnitude. The specific exchange current densities of polished electrodes presented here are generally

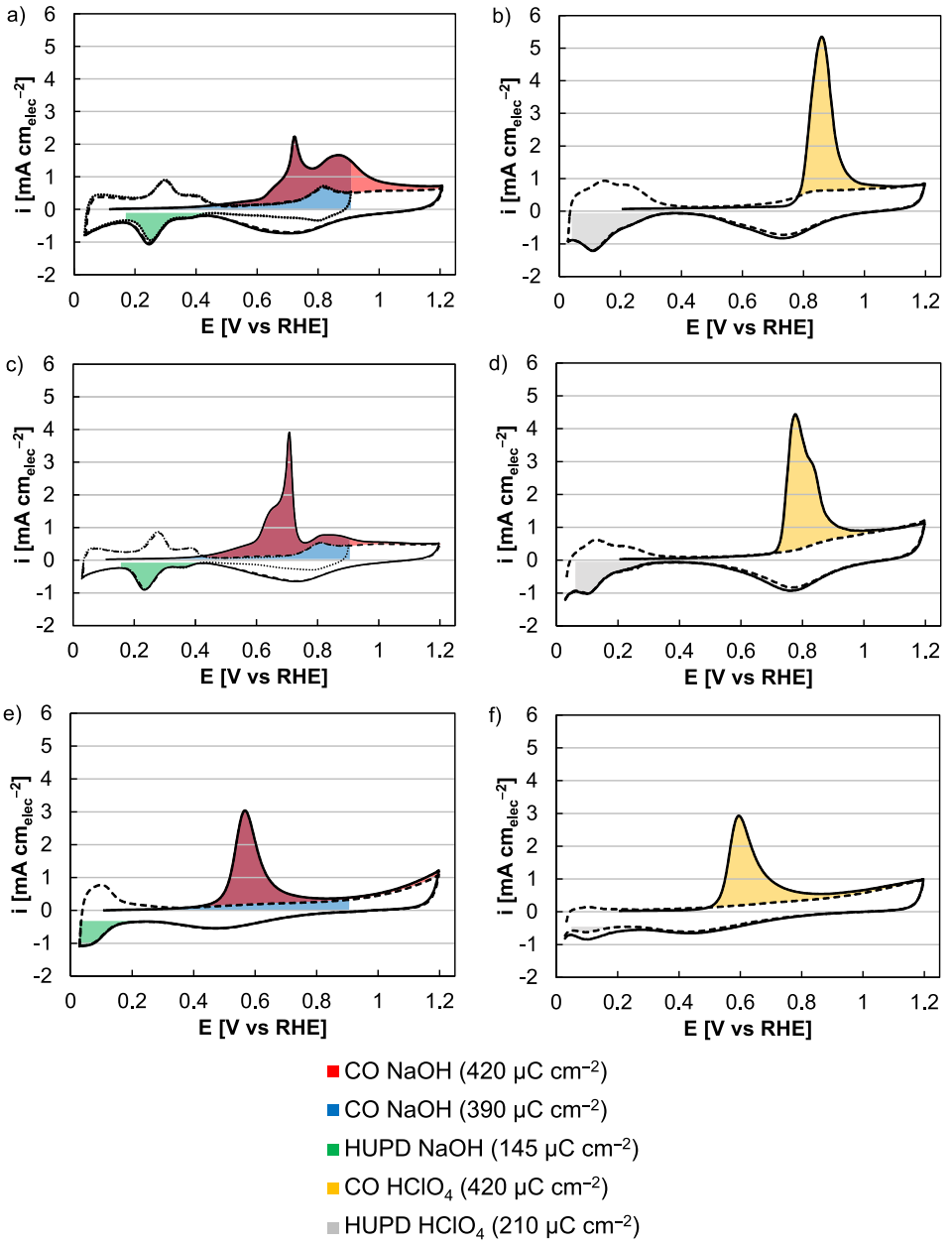

Figure 6. Carbon monoxide stripping and cyclic voltammograms of (a−b) Pt/HSC, (c−d) Pt/Vu, and (e−f) PtRu/Vu, in 0.1 M (a,c,e) sodium hydroxide and (b,d,f) perchloric acid. ECAs were determined in 0.1 M sodium hydroxide by carbon monoxide stripping using cyclic voltammograms as a background subtraction (CO NaOH, 420 μC cm^{-2}, red)[42] and a fixed potential window (CO NaOH, 390 μC cm^{-2}, blue),[43] and hydrogen underpotential deposition (HUPD NaOH, 145 μC cm^{-2}, green).[43] ECAs were determined in 0.1 M perchloric acid by carbon monoxide stripping using cyclic voltammograms as a background subtraction (CO HClO$_4$, 420 μC cm^{-2}, yellow)[42] and hydrogen underpotential deposition (HUPD HClO$_4$, 210 μC cm^{-2}, gray).[44]

comparable to or exceed the activities published elsewhere, potentially due to electrolyte purity and conditioning protocols. In certain instances, however, nanoparticle-based materials outperformed the activity of the Pt and Pt-Ru baselines (Pt/HSC from Tanaka Kikinzoku Kogyo TEC10E50E and PtRu/Vu from Alfa Aesar 44172), which may be due to differences between the individual catalysts.

A number of testing choices were made that influenced half-cell performance. Pt and Pd catalysts were electrochemically conditioned in 0.1 M perchloric acid (50 cycles, 0.025−1.0 V) to clean the surface, which improved surface area and HER-HOR activity; afterwards, the electrode tips were rinsed in water and conditioned in alkaline electrolytes prior to activity evaluations. Pt-Ru, however, was not conditioned in acid since these protocols led to Ru dissolution and lower performance. Particular care was taken with Pd conditioning, and Pd catalysts were not exposed to less than −0.1 V to avoid subsurface hydride formation. Conversely, Ni catalysts were conditioned at negative potential (−0.4−0.0 V) to limit the impact of the surface oxide layers, and because higher HER performance was observed if the catalyst did not spend extended time at elevated potential.

Ni conditioning can have a significant impact on HER performance, either due to extended time spent at low potential forming Ni hydrides or at high potential forming Ni oxides (Figure 2). Although Ni nanoparticle conditioning at negative potential was used in this study (10 cycles, −0.4−0.0 V), it resulted in identical performance to the catalyst when unconditioned. Conditioning at a more negative potential, however, resulted in positive current above 0 V, likely due to the oxidation of formed surface hydrides. The positive current, however, only persisted for a few cycles and the original HER polarization curve could be reproduced. Conversely, conditioning to elevated potential produced larger negative current in the cyclic voltammograms, likely due to the reduction of formed surface oxides. Although the original HER polarization curves could be reproduced in most cases, conditioning at 1.2 V for ≥ 10 min resulted in slightly lower performance that could not be recovered without reconditioning at negative potential. Conditioning can also significantly affect Pd performance, where exposure to excessive negative potential appeared to form hydrides and positive current above 0 V that in cases was more difficult to remove.

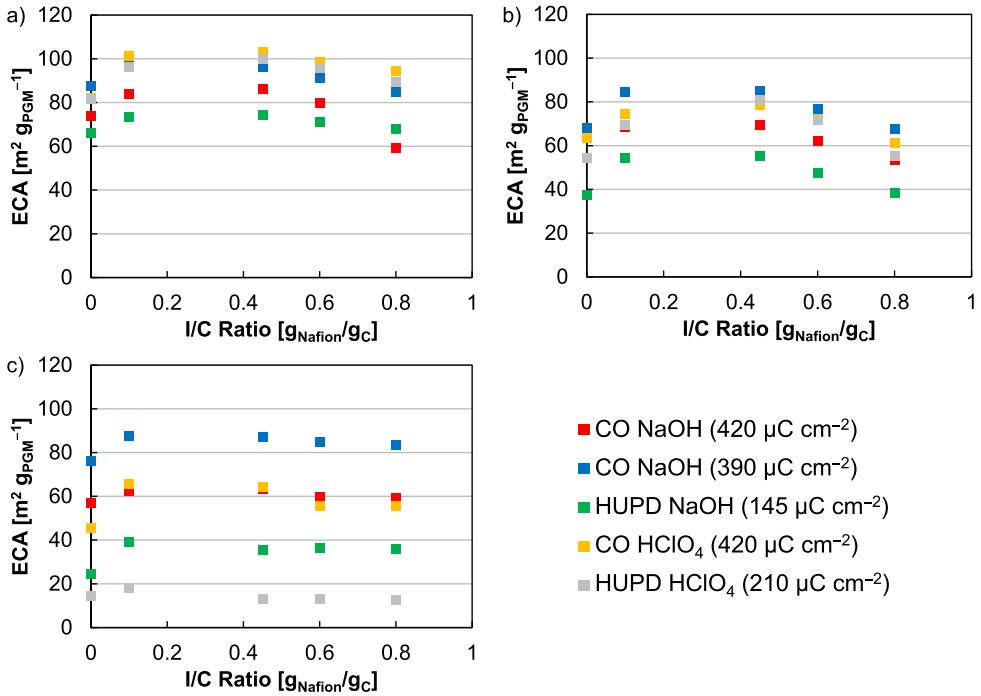

Figure 7. Electrochemical surface areas of (a) Pt/HSC, (b) Pt/Vu, and (c) PtRu/Vu, determined by carbon monoxide stripping and hydrogen underpotential deposition. ECAs were determined in 0.1 M sodium hydroxide by carbon monoxide stripping using cyclic voltammograms as a background subtraction (CO NaOH, 420 μC cm^{-2}, red)[42] and a fixed potential window (CO NaOH, 390 μC cm^{-2}, blue),[43] and hydrogen underpotential deposition (HUPD NaOH, 145 μC cm^{-2}, green).[43] ECAs were determined in 0.1 M perchloric acid by carbon monoxide stripping using cyclic voltammograms as a background subtraction (CO $HClO_4$, 420 μC cm^{-2}, yellow)[42] and hydrogen underpotential deposition (HUPD $HClO_4$, 210 μC cm^{-2}, gray).[44]

The electrolyte manufacturer and purity was found to impact the observed HER-HOR performances (Figure 3). Markovic et al. among others have examined electrolyte impurities and demonstrated an effect on Pt HER-HOR.[31] The focus of this study was to minimize impurity impacts by evaluating a number of commercially available electrolytes and to produce robust performance baseline. The choice of electrolyte tended to more strongly influence polished metal electrodes and higher performing PGMs, and the activity of a polished Pt electrode was the most affected by changes to the electrolyte. Manufacturer specifications were examined for potential causes in variable HER-HOR performance, however this was somewhat complicated by data availability and the contaminant ranges specified. In general, however, higher activity tended to correspond to lower contaminant levels. An exception was the amount of sodium or potassium carbonate reported, which did not align to these activity trends. Since the evaluated chemicals contained low amounts of carbonate ($\leq 2\%$), small differences may be mitigated by air exposure prior to testing (10−12 minutes to weigh, dissolve, deaerate, and test) or may be less critical than other contaminant levels. For nanoparticle catalysts, electrolyte purity effects generally tended to be smaller, similar to previous findings in Pt-oxygen reduction baselines in acidic RDE half-cells.[84] While the effect was smaller for the commercial nanoparticles evaluated, contaminant effects may be larger at lower catalyst loading or for catalysts with lower surface area.

The performances found in this study on a polished Pt electrode were compared to published values in literature (Table II). These types of comparisons are complicated since: researchers rarely specify the product used to make electrolytes; and electrolyte impurity is not the only source of contamination or the only reason behind performance differences. The comparison, however, illustrates the need for established best practices in the testing of HER-HOR catalysts.

TraceSELECT sodium hydroxide (Honeywell Research Chemicals) was used throughout the remainder of this publication, since it produced HER-HOR activity on a polished Pt electrode representative of higher purity electrolytes. A 0.1 M concentration was also used since it produced optimal performance, rationalized as a balance between hydroxide abundance resisting carbonation and contaminants competing for Pt sites (hydroxide itself or impurities, Figure 4).

Ink optimization was investigated by varying ionomer content and electrode loading, to find peak PGM performance (Figure 5). Trends observed while varying the amount of ionomer included: a specific activity drop with increasing ionomer content; and surface area peaking at moderate ionomer amounts (I:C of 0.1−0.6). Low ionomer content resulted in low surface area and high specific activity, attributed to a combination of poorly dispersed inks (low surface area) and minimal ionomer contamination (high specific activity). High ionomer

Table III. Comparison of the specific exchange current densities of a polished Pt electrode in half-cell durability tests using polytetrafluoroethylene (PTFE) and glass cells to a previous study examining glass contamination.

Author	Ref.	Cell	Time	$i_{0,s}$ [mA cm_M^{-2}]
This work		PTFE	0	1.21
This work		PTFE	27 min	1.01
This work		PTFE	1 wk	0.289 (1.18)[a]
This work		Glass	0	1.21
This work		Glass	27 min	1.01
This work		Glass	1 wk	0.242 (1.17)[a]
Mayrhofer and Arenz et al.	28	Glass[b]	0	0.430[c]
Mayrhofer and Arenz et al.	28	Glass[b]	15 min	0.0428[c]

[a]Two values for the specific exchange current density were provided, the first in the original electrolyte and the second (in parentheses) in a fresh electrolyte.
[b]Experiments were conducted by Mayrhofer and Arenz et al. in a PTFE cell with simulated glass contamination.
[c]Exchange current densities were approximated by the Butler-Volmer equation assuming an anodic charge transfer coefficient of 0.5.

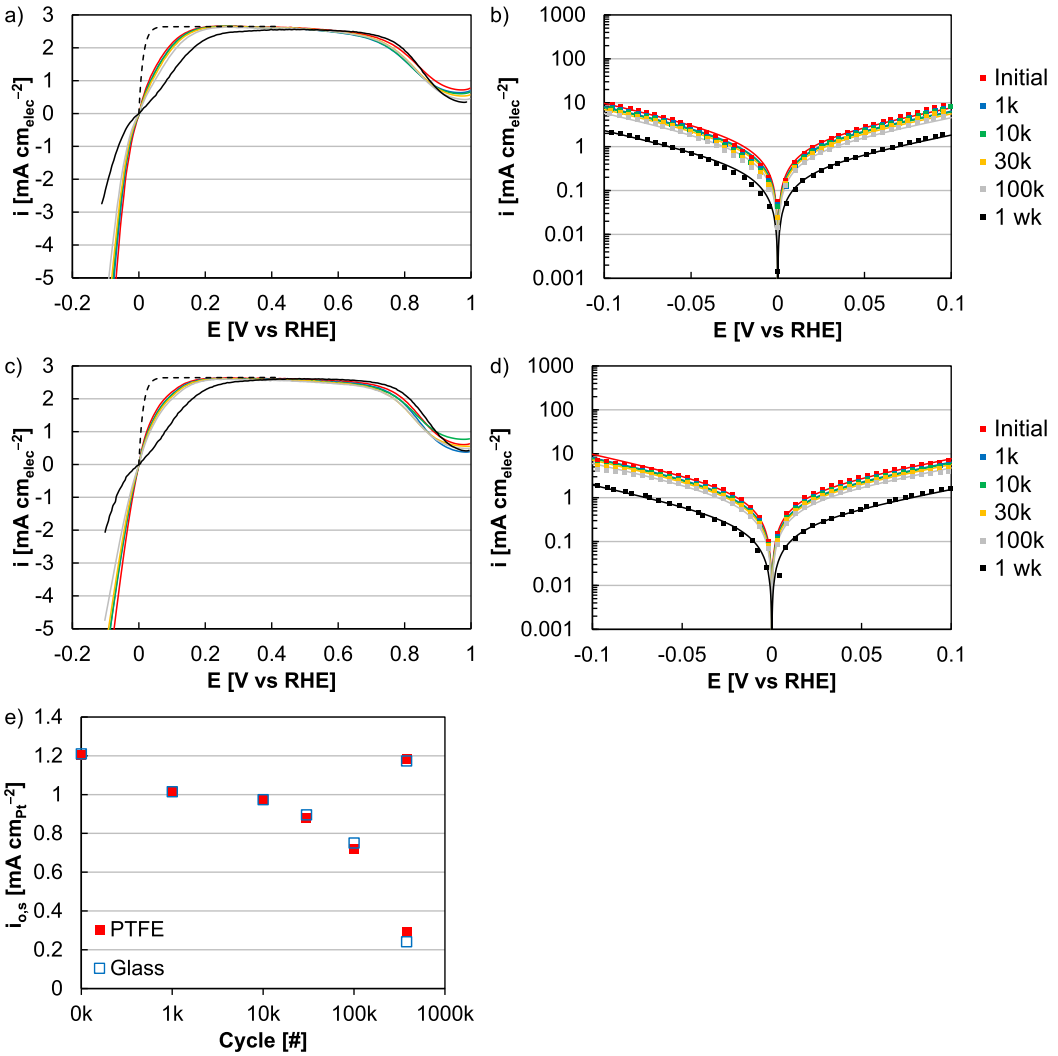

Figure 8. (a,c) Polarization curves and (b,d) Butler-Volmer fits of a polished Pt electrode using (a−b) polytetrafluoroethylene and (c−d) glass electrochemical cells. Polarization curves were taken cathodically at 10 mV s^{-1} and 2500 rpm using a 0.1 M NaOH electrolyte (TraceSELECT, Honeywell Research Chemicals). The dashed black line (a, c) is the Nernstian diffusion limited overpotential. (e) Summary of mass (red) and specific (blue) exchange current densities for polytetrafluoroethylene (PTFE, red) and glass (blue). The two values for 1 wk corresponded to experiments in the original (low values) and fresh (high values) electrolyte.

amounts, however, resulted in both low surface area and specific activity, attributed to the larger ionomer content blocking catalyst sites, which in cases (I:C of 0.8) resulted in a visible sheen covering the electrode. Nafion ionomer was used in this study to optimize inks. While Nafion is inappropriate in AEM devices, the alkaline electrolyte provides abundant hydroxide conductivity and the ionomer's primary purpose in half-cell tests is to promote ink uniformity and coating quality. The Nafion ionomer resulted in electrodes with higher HER-HOR performance compared to commercial (Tokuyama AS-4) and novel AEM-based ionomers, and performance differences may be due to the relative contaminate effects of these ionomers (ammonium-, imidazolium-, phosphonium-based compounds).[26,85] At lower catalyst loading, it was also found that higher mass-normalized exchange current densities could be produced. Moderate PGM loadings (17.8 μg cm_{elec}^{-2}), however, were used in the baseline evaluations since they reached full diffusion limited currents without the complications of high loading, including the early onset of HER transport limitations, reaching the Nernstian diffusion limited overpotential (HOR), and underutilizing the catalyst layer.

In this study, carbon monoxide oxidation was used to evaluate the ECAs of Pt and Pt-Ru catalysts, using a Coulombic charge of 420 μC cm_{Pt}^{-2} (Figures 6 and 7). Since this method is not universally applied throughout literature, a number of other approaches were evaluated and include different charge correction factors, fixed potential limits, and hydrogen underpotential deposition.[43,86,87] This effort was completed to explain why carbon monoxide oxidation (420 μC cm_{Pt}^{-2}) was used in this study, and since differences in ECA determinations have an obvious impact on reported specific activities. Carbon monoxide stripping can be somewhat complicated in alkaline electrolytes, since hydroxide abundance produces heterogeneous hydroxide adsorption and a range of stripping potentials. Methods have been developed for charge integration over a fixed range, which simplify the calculation and produce reasonable surface areas on Pt electrodes.[43] These methods, however, do not account for differences in support capacitance and may need to be recalibrated with changes in catalyst type (PtRu/Vu). Similarly, hydrogen underpotential deposition can be useful in determining Pt surface areas, but is less effective on PtRu/Vu. While carbon monoxide stripping voltammograms on Pt in base occur over a wide potential range, this method (carbon monoxide oxidation, 420 μC cm_{Pt}^{-2}) was used to calculate ECAs and specific exchange current densities in this study since it produced reasonable values for each of the Pt-based catalysts evaluated (Pt, Pt/HSC, Pt/Vu, PtRu/Vu).

In addition to the test choices of electrolyte, conditioning protocol, and ink composition, the catalyst itself has obvious impacts

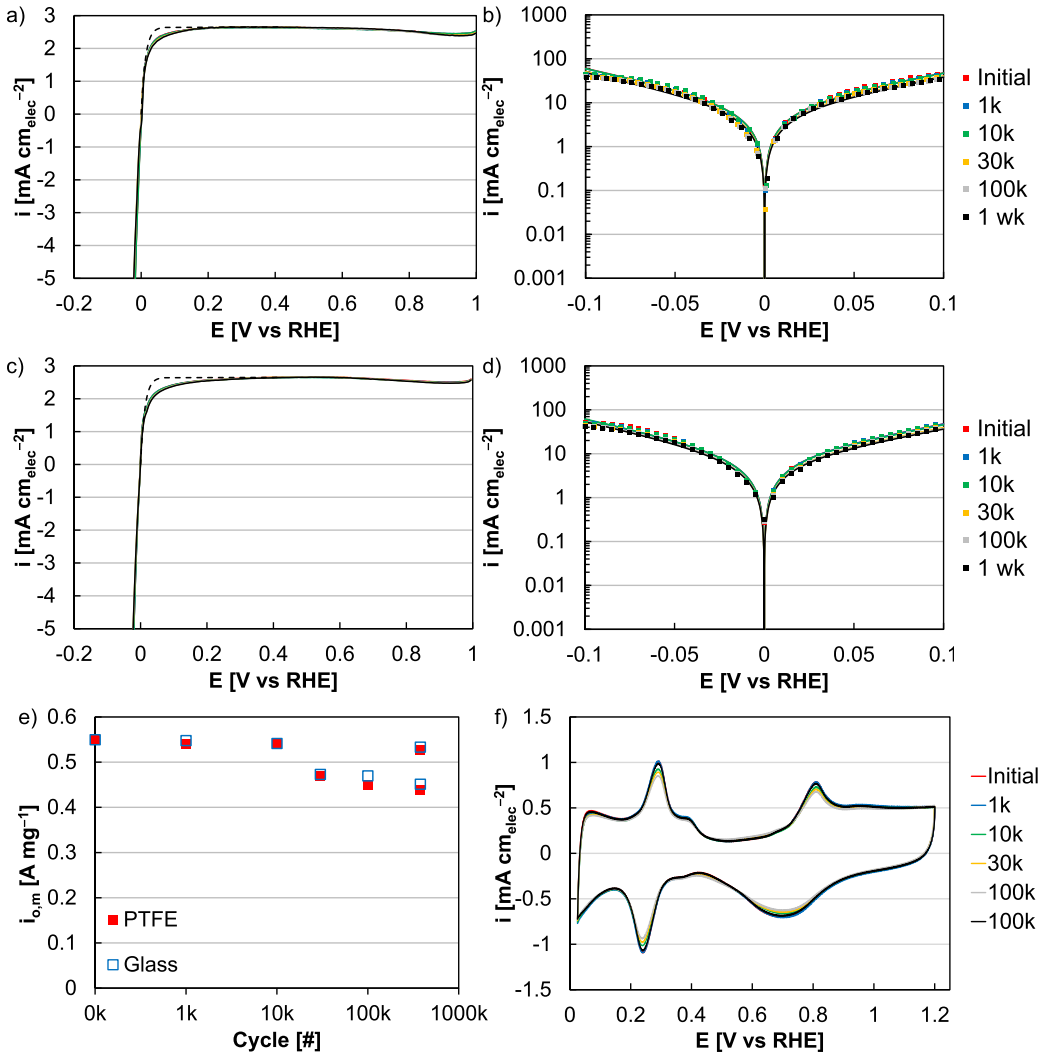

Figure 9. (a,c) Polarization curves and (b,d) Butler-Volmer fits of Pt/HSC using (a−b) polytetrafluoroethylene and (c−d) glass electrochemical cells. Polarization curves were taken cathodically at 10 mV s^{-1} and 2500 rpm using a 0.1 M NaOH electrolyte (TraceSELECT, Honeywell Research Chemicals). The dashed black line (a, c) is the Nernstian diffusion limited overpotential. (e) Summary of mass exchange current densities for polytetrafluoroethylene (PTFE, red) and glass (blue). The two values for 1 wk corresponded to experiments in the original (low values) and fresh (high values) electrolyte. (f) Cyclic voltammograms of Pt/HSC following cycling in the potential range −0.2−0.2 V vs. RHE. The two voltammograms for 100,000 cycles corresponded to experiments in the original (gray) and fresh (black) electrolyte.

on the observed performance. Surface structure, including particle size, lattice spacing, faceting, and coordination number may have a significant effect on the HER-HOR activity of materials. Additional effects including alloying (lattice spacing) and bifunctionality (oxophilicity) may modify catalyst reactivity and have been previously presented as routes to develop catalysts.[1,66] Previous studies have confirmed activity differences on low-index Pt facets and a Pd particle size effects; these conclusions, however, are not universally agreed upon in literature and studies have not been completed systematically for the other materials evaluated here (Pt-Ru, Ni).[25,72,88] Differences between the specific exchange current densities of nanoparticle catalysts and polished electrodes in this study, however, suggest that a particle size effect is plausible for Pt, Pd, and Ni (Figure 1).

Electrochemical cell material.—Durability tests were completed on Pt/HSC and a polished Pt electrode to determine whether half-cell durability tests were viable in alkaline electrolytes, and whether polytetrafluoroethylene electrochemical cells were necessary to avoid contaminant-based performance loss. Mayrhofer and Arenz et al. among others have previously demonstrated the impact of glass corrosion and related contaminants on performance evaluations.[28,30] While aspects of this issue have previously been presented, it required that the working electrode only saw low potential ($\leq$ 0.5 V). This study used typical testing conditions (10 cycles, −0.1−1.0 V prior to each HER-HOR polarization curve) to evaluate whether polytetrafluoroethylene cells were truly necessary to evaluate catalyst performance and durability in RDE half-cells.

Durability cycles were completed in the potential range −0.2−0.2 V (anticipated operation range in reversible fuel cells) up to 100,000 cycles (44.4 h). Electrolytes were also aged for 1 wk in glass and polytetrafluoroethylene cells under continual hydrogen flow, to test the furthest extent of this comparison. While loss was observed on a polished Pt electrode, these losses were similar in either electrochemical cell and were rationalized as either carbonation affecting electrolyte composition or electrolyte impurities adsorbing onto the working electrode over time (Figure 8). Although glass corrosion and glass-related contaminant adsorption appear to be highly impactful when the electrode only sees low potential ($\leq$ 0.5 V),[28,30] polytetrafluoroethylene and glass cells produced similar performance and durability results when the electrode was evaluated with typical test conditions (−0.1−1.0 V). Since performance decreases were observed for polytetrafluoroethylene and glass cells alike, the loss was

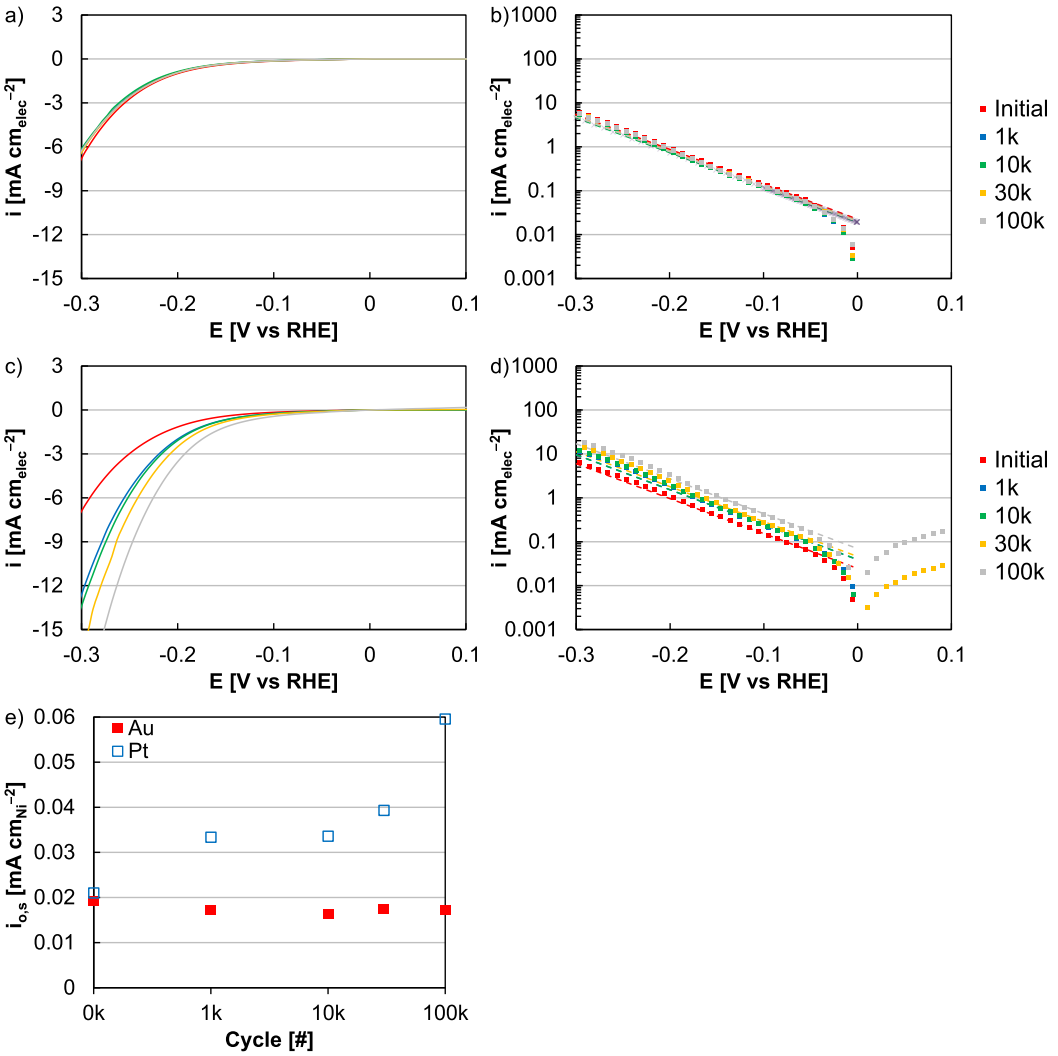

Figure 10. (a,c) Polarization curves and (b,d) Butler-Volmer fits of a polished Ni electrode using (a−b) Au and (c−d) Pt counter electrodes. Polarization curves were taken cathodically at 10 mV s^{-1} and 2500 rpm using a 0.1 M NaOH electrolyte (TraceSELECT, Honeywell Research Chemicals) in polytetrafluoroethylene cells. (e) Summary of specific exchange current densities for a polished Ni electrode using Au (red) and Pt (blue) counter electrodes.

likely due to carbonation and contaminants inherent to the electrolyte and not dramatically affected by the addition of contaminants due to glass dissolution.

Care was taken in these tests to ensure that the polytetrafluoroethylene cell contained no glass, including in the reference electrode (felt tip, plastic body), Luggin capillary, and bubbler. While continual gas flow mitigated carbonation effects, loss could not be prevented. Alternative electrochemical cells may accentuate or minimize these losses, and design aspects of the tested cells may reduce air exposure, including an extended cell neck (glass) and tight electrode fittings (polytetrafluoroethylene). The glass composition (impurity species and quantity) may also impact performance and performance changes over time.

The results found in this study using polytetrafluoroethylene and glass cells were compared to the work of Mayrhofer and Arenz et al. who previously demonstrated the impact of glass corrosion and related contaminants on performance evaluations (Table III).[28] Although there may have been differences between the projected and actual amount of contaminants in the electrolyte, electrode conditioning (10 cycles, −0.1–1.0 V prior to each HER-HOR polarization curve) likely plays a significant role and may be necessary to acquire accurate and reproducible performance.

While significant loss was observed in the testing of a polished Pt electrode, these performance losses were less severe for Pt/HSC and corresponded to 14% after 30,000 cycles (20% after 1 wk, Figure 9). In both cases the losses could be recovered with testing in a fresh electrolyte (Figures 8e and 9e).

From these results, two conclusions were made. First, half-cell accelerated stress tests gave reasonable results for Pt durability, in that no loss was expected in the examined potential range (−0.2−0.2 V).[37] Since fresh electrolyte replacement resulted in no performance losses, the observed losses could have been due to electrolyte deterioration (carbonation) or the adsorption of contaminants (within the electrolyte) over time onto the working electrode. While electrolyte losses were less severe for Pt/HSC, they may be significantly larger for catalysts with lower surface area or at lower loading. Secondly, the electrochemical cell material (glass versus polytetrafluoroethylene) did not appear critical in testing, and these configurations gave similar results in initial and post-durability performance. Polytetrafluoroethylene cells can potentially be advantageous after extended use, since glass etching may increase the cell surface area and increase dissolution rates over time. Alternatively, glass cells can potentially be advantageous in novel catalyst testing where electrochemical conditioning is needed to remove less active metals, ligands, and impurities, since glass cells can potentially be cleaned more effectively than polytetrafluoroethylene.

Extended operation may have a significant effect on electrocatalyst performance, depending on the device of interest and the potential

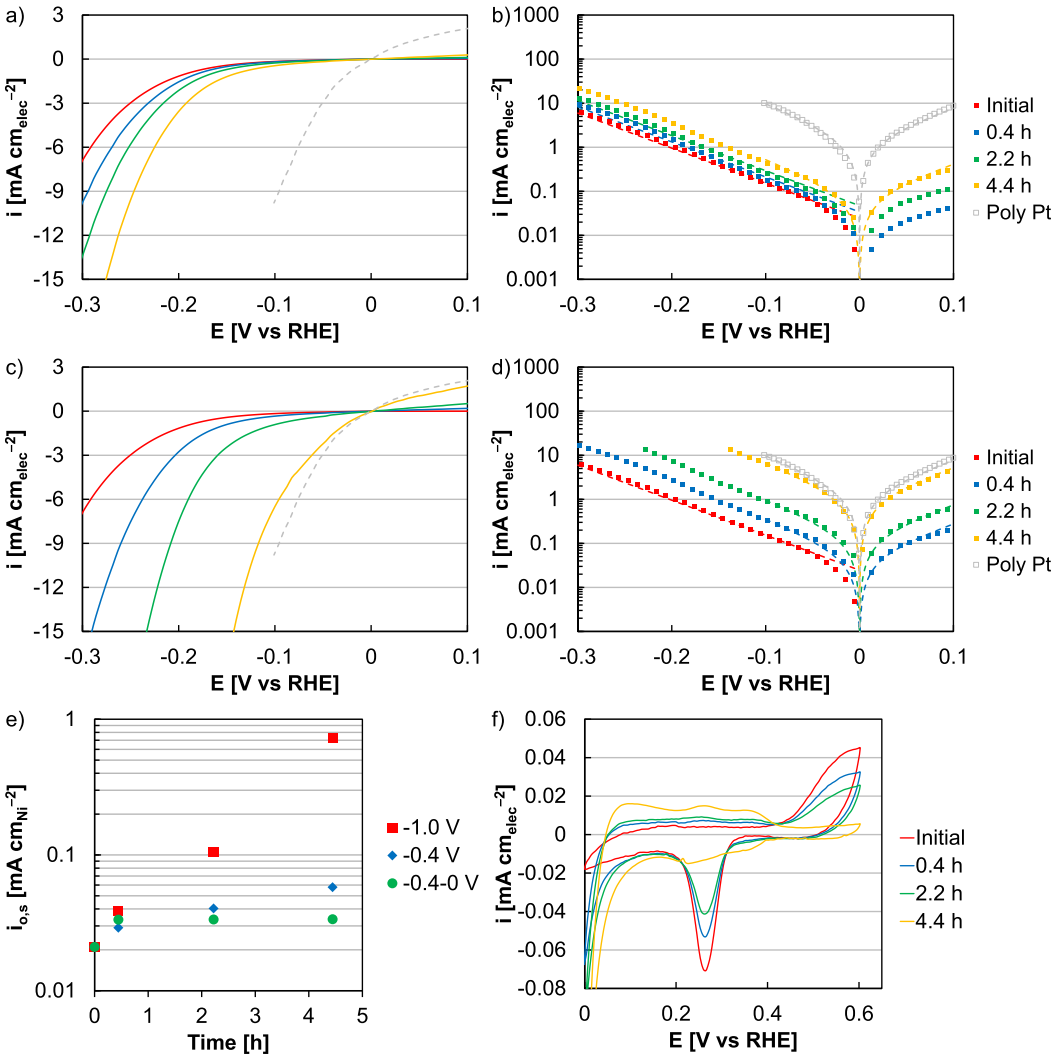

Figure 11. (a,c) Polarization curves and (b,d) Butler-Volmer fits of a polished Ni electrode held at (a−b) −0.4 V and (c−d) −1.0 V using Pt counter electrodes. Polarization curves were taken cathodically at 10 mV s^{-1} and 2500 rpm using a 0.1 M NaOH electrolyte (TraceSELECT, Honeywell Research Chemicals) in polytetrafluoroethylene cells. (e) Summary of specific exchange current densities for a polished Ni electrode: held at −1.0 V (red), held at −0.4 V (blue), and cycled between −0.4−0.0 V (green). (f) Cyclic voltammograms of a polished Ni electrode following holds at −1.0 V. Each test used a Pt counter electrode.

range explored. Surface structure, including particle size, lattice spacing, faceting, and coordination number may not be affected equally and can result in differences between the durabilities of individual catalysts. In this case, however, a potential range of −0.2−0.2 V vs. RHE was probed to baseline HER-HOR catalysts intended as hydrogen electrodes in AEM electrolyzers and fuel cells. Since durability testing at these potentials did not reach Pt redox or dissolution, minimal loss was expected and found.[37] A slight decrease was observed in Pt/HSC performance after 1 wk; since this loss was recovered upon using a fresh electrolyte, the loss was attributed to electrolyte deterioration. Slight changes were also observed in Pt/HSC cyclic voltammograms and carbon monoxide voltammograms after 100,000 cycles (increase in capacitance, decrease in Pt surface features). Since these changes largely disappeared when the catalyst was retested with a fresh electrolyte, they were likely not due to Pt loss or growth.

Counter electrode material.—Potential cycling (−0.4−0 V) was completed on a polished Ni electrode, using Pt and Au counter electrodes, to evaluate the effect of the counter electrode on activity and durability evaluations (Figure 10). These experiments were completed with the aim of quantifying the impact of Pt counter electrode dissolution on non-PGM performance. While Pt dissolution concerns at elevated potential are obvious and addressed elsewhere, many recent non-PGM HER studies use Pt counters. This work uses electrochemical conditioning procedures adapted from literature to quantify how test choice can overestimate non-PGM HER kinetics.

While both configurations produced comparable initial performance (first polarization curve), the results quickly deviated and a Pt counter electrode improved Ni performance 60% within 30 min (1000 cycles). This improvement was rationalized as Pt deposition on the working electrode increasing activity.[29,37] With a lower bound of −0.4 V, a polished Ni electrode routinely produced currents in excess of 2 mA, pushing the counter electrode (Pt mesh, 125 cm^2 approximated by hydrogen underpotential deposition) to potentials above 2.5 V. Although polycrystalline Ni initially produced no HOR activity, small amounts of activity were observed after extended operating times (30,000 cycles, 13.5 h). In the case of Au, the counter electrode also saw high potentials (≥ 2.5 V) and may have deposited on the Ni working electrode. A performance benefit, however, was likely mitigated since Ni and Au have comparable HER activity, and the use of a carbon counter electrode produced similar results. Although Au did not improve Ni activity in this case, it may improve performance when testing catalysts less active for HER.

Potential holds at −0.4 and −1.0 V were also completed on polished Ni electrodes, using Pt counter electrodes, to evaluate the extent that counter electrode plating could improve Ni performance

(Figure 11). These tests were limited by time (4.4 h, time equivalent to 10,000 cycles −0.4−0 V) and potential (≥ −1.0 V) to focus on possible gains through catalyst conditioning and to not damage the counter electrode. Greater time spent at more negative potential resulted in larger performance improvements, and these improvements increased in the order −0.4−0.0 V cycle < −0.4 V hold < −1.0 V hold. Following 4.4 h at −1.0 V, significant HOR activity was observed on Ni, and the HER-HOR exchange current density was within 80% of polycrystalline Pt. Additional factors may influence the potential at the counter electrode and its dissolution rate, including the ECA of the counter and the performance of the working electrode (intrinsic activity, loading, ECA). In any case, the use of a Pt counter is not ideal, as the metal is highly active for HER-HOR and susceptible to dissolution (plating) at working electrode-relevant test conditions. These results are of concern since many non-PGM HER catalyst evaluations still use Pt counter electrodes, and on occasion, use highly negative potentials during electrochemical conditioning. It appears prudent to use materials in the electrochemical cell that are less active than the catalyst of interest, to ensure confidence in the measurement.

Conclusions

Polished metal electrodes and commercial catalysts (Pt, Pt-Ru, Pd, and Ni) were evaluated for HER-HOR activity in RDE half-cells. A number of testing choices, including electrolyte purity, ink composition, electrochemical cell material, and counter electrode material were evaluated to quantify the effect of protocols on half-cell performance and durability. Electrolyte manufacturer produced a range of activities, which generally correlated to contaminant levels; these electrolyte effects, however, tended to be stronger for polished metal electrodes than nanoscale catalysts. Ink composition impacted commercial catalyst activity, and moderate ionomer content (I:C 0.1−0.6) was needed to balance dispersion quality and contaminant effects.

Minimal performance differences were found when comparing glass and polytetrafluoroethylene electrochemical cells, either initially or following electrolyte aging, and durability losses were driven by electrolyte deterioration. These losses were small for nanoscale catalysts (Pt/HSC, 14% after 30,000 cycles), suggesting that alkaline durability tests are viable provided they have a limited timeframe and the electrolyte is refreshed prior to activity evaluations. The choice of counter electrode also impacted performance, and a Pt counter improved Ni activity, significantly when cycling at modest negative potential (x3 improvement, 100,000 cycles, −0.4−0.0 V) or extremely when holding at high negative potential (x35 improvement, 4.4 h, −1.0 V). The degree of benefit may change under reasonable circumstances, including catalyst differences at the working electrode (intrinsic activity, loading, ECA), higher overpotential, lower surface area counters, or incidental current excursions.

RDE half-cells are typically used to evaluate the kinetic capabilities of different catalysts and gauge their relative performance. Establishing performance baselines is critical for setting realistic expectations, particularly in the absence of device testing, when RDE half-cell activity can be used to infer MEA performance. Wider implementation of performance baselines is needed, particularly when comparing PGM and non-PGM activity, and when assessing the benefit of catalyst developments.

Acknowledgments

This work was supported by the Laboratory Directed Research and Development (LDRD) Program at the National Renewable Energy Laboratory. NREL is a national laboratory of the U.S. Department of Energy, Office of Energy Efficiency and Renewable Energy, operated by the Alliance for Sustainable Energy, LLC.

ORCID

Shaun M. Alia https://orcid.org/0000-0002-7647-9383

References

1. J. K. Nørskov, T. Bligaard, A. Logadottir, J. R. Kitchin, J. G. Chen, S. Pandelov, and U. Stimming, *J. Electrochem. Soc.*, **152**, J23 (2005).
2. J. Greeley, T. F. Jaramillo, J. Bonde, I. Chorkendorff, and J. K. Norskov, *Nat. Mater*, **5**, 909 (2006).
3. W. Sheng, M. Myint, J. G. Chen, and Y. Yan, *Energy Environ. Sci.*, **6**, 1509 (2013).
4. D. Strmcnik, M. Uchimura, C. Wang, R. Subbaraman, N. Danilovic, D. Van Der Vliet, A. P. Paulikas, V. R. Stamenkovic, and N. M. Markovic, *Nature chemistry*, **5**, 300 (2013).
5. Y. Wang, G. Wang, G. Li, B. Huang, J. Pan, Q. Liu, J. Han, L. Xiao, J. Lu, and L. Zhuang, *Energy Environ. Sci.*, **8**, 177 (2015).
6. J. Durst, A. Siebel, C. Simon, F. Hasche, J. Herranz, and H. Gasteiger, *Energy Environ. Sci.*, **7**, 2255 (2014).
7. J. N. Schwämmlein, H. A. El-Sayed, B. M. Stühmeier, K. F. Wagenbauer, H. Dietz, and H. A. Gasteiger, *ECS Trans.*, **75**, 971 (2016).
8. S. St. John, R. W. Atkinson III, R. R. Unocic, T. A. Zawodzinski Jr, and A. B. Papandrew, *J. Phys. Chem. C*, **119**, 13481 (2015).
9. R. Kavian, S.-I. Choi, J. Park, T. Liu, H.-C. Peng, N. Lu, J. Wang, M. J. Kim, Y. Xia, and S. W. Lee, *Journal of Materials Chemistry A*, **4**, 12392 (2016).
10. S. M. Alia, B. S. Pivovar, and Y. Yan, *J. Am. Chem. Soc.*, **135**, 13473 (2013).
11. M. Gong, W. Zhou, M.-C. Tsai, J. Zhou, M. Guan, M.-C. Lin, B. Zhang, Y. Hu, D.-Y. Wang, and J. Yang, *Nature communications*, **5** (2014).
12. J. Staszak-Jirkovský, C. D. Malliakas, P. P. Lopes, N. Danilovic, S. S. Kota, K.-C. Chang, B. Genorio, D. Strmcnik, V. R. Stamenkovic, and M. G. Kanatzidis, *Nature materials*, **15**, 197 (2016).
13. W. Sheng, A. P. Bivens, M. Myint, Z. Zhuang, R. V. Forest, Q. Fang, J. G. Chen, and Y. Yan, *Energy Environ. Sci.*, **7**, 1719 (2014).
14. J. Yin, Q. Fan, Y. Li, F. Cheng, P. Zhou, P. Xi, and S. Sun, *J. Am. Chem. Soc.*, **138**, 14546 (2016).
15. D. Voiry, H. Yamaguchi, J. Li, R. Silva, D. C. Alves, T. Fujita, M. Chen, T. Asefa, V. B. Shenoy, and G. Eda, *Nature materials*, **12**, 850 (2013).
16. E. J. Popczun, C. G. Read, C. W. Roske, N. S. Lewis, and R. E. Schaak, *Angew. Chem.*, **126**, 5531 (2014).
17. D. Kong, H. Wang, Z. Lu, and Y. Cui, *J. Am. Chem. Soc.*, **136**, 4897 (2014).
18. M. A. Lukowski, A. S. Daniel, F. Meng, A. Forticaux, L. Li, and S. Jin, *J. Am. Chem. Soc.*, **135**, 10274 (2013).
19. H. Jin, J. Wang, D. Su, Z. Wei, Z. Pang, and Y. Wang, *J. Am. Chem. Soc*, **137**, 2688 (2015).
20. T. Liu, Q. Liu, A. M. Asiri, Y. Luo, and X. Sun, *Chem. Commun.*, **51**, 16683 (2015).
21. J. M. McEnaney, T. L. Soucy, J. M. Hodges, J. F. Callejas, J. S. Mondschein, and R. E. Schaak, *Journal of Materials Chemistry A*, **4**, 3077 (2016).
22. J. Jiang, M. Gao, W. Sheng, and Y. Yan, *Angew. Chem.*, **128**, 15466 (2016).
23. P. Jiang, Q. Liu, and X. Sun, *Nanoscale*, **6**, 13440 (2014).
24. K. C. Neyerlin, W. Gu, J. Jorne, and H. A. Gasteiger, *J. Electrochem. Soc.*, **154**, B631 (2007).
25. W. Sheng, H. A. Gasteiger, and Y. Shao-Horn, *J. Electrochem. Soc.*, **157**, B1529 (2010).
26. B. Pivovar, *Advanced Ionomers and MEAs for Alkaline Membrane Fuel Cells*, in, U. S. Department of Energy Editor, https://www.hydrogen.energy.gov/pdfs/review16/fc147_pivovar_2016_o.pdf (2016).
27. J. X. Wang, in *Encyclopedia of Applied Electrochemistry*, p. 1045, Springer (2014).
28. K. Mayrhofer, G. Wiberg, and M. Arenz, *J. Electrochem. Soc.*, **155**, P1 (2008).
29. S. Cherevko, A. R. Zeradjanin, G. P. Keeley, and K. J. Mayrhofer, *J. Electrochem. Soc.*, **161**, H822 (2014).
30. K. Mayrhofer, A. Crampton, G. Wiberg, and M. Arenz, *Journal of the Electrochemical Society*, **155**, P78 (2008).
31. R. Subbaraman, N. Danilovic, P. P. Lopes, D. Tripkovic, D. Strmcnik, V. R. Stamenkovic, and N. M. Markovic, *J. Phys. Chem. C*, **116**, 22231 (2012).
32. A. Milbrandt and M. Mann, in, U. S. Department of Energy Editor, http://www.nrel.gov/docs/fy09osti/42773.pdf (2009).
33. H2 at Scale: Deeply Decarbonizing our Energy System, in, U. S. Department of Energy Editor, https://www.hydrogen.energy.gov/pdfs/review16/2016_amr_h2_at_scale.pdf (2016).
34. Hydrogen at Scale: Deeply Decarbonizing Our Energy System, in, U. S. Department of Energy Editor, https://www.hydrogen.energy.gov/pdfs/htac_apr16_10_pivovar.pdf (2016).
35. B. Pivovar, Hydrogen at Scale: Deeply Decarbonizing our Energy System, in, U. S. Department of Energy Editor, https://www.energy.gov/sites/prod/files/2016/07/f33/fcto_webinarslides_h2_at_scale_072816.pdf (2016).
36. I. C. Man, H. Y. Su, F. Calle-Vallejo, H. A. Hansen, J. I. Martínez, N. G. Inoglu, J. Kitchin, T. F. Jaramillo, J. K. Nørskov, and J. Rossmeisl, *ChemCatChem*, **3**, 1159 (2011).
37. M. Pourbaix, *Atlas of electrochemical equilibria in aqueous solutions*, National Association of Corrosion Engineers, Houston, Texas (1974).
38. P. J. Rheinländer, J. Herranz, J. Durst, and H. A. Gasteiger, *J. Electrochem. Soc.*, **161**, F1448 (2014).
39. C. C. McCrory, S. Jung, I. M. Ferrer, S. M. Chatman, J. C. Peters, and T. F. Jaramillo, *J. Am. Chem. Soc.*, **137**, 4347 (2015).
40. B. E. Conway and L. Bai, *Journal of the Chemical Society, Faraday Transactions 1: Physical Chemistry in Condensed Phases*, **81**, 1841 (1985).
41. S. A. Machado and L. Avaca, *Electrochim. Acta*, **39**, 1385 (1994).
42. T. Ralph, G. Hards, J. Keating, S. Campbell, D. Wilkinson, M. Davis, J. St-Pierre, and M. Johnson, *J. Electrochem. Soc.*, **144**, 3845 (1997).
43. F. J. Vidal-Iglesias, R. M. Arán-Ais, J. Solla-Gullón, E. Herrero, and J. M. Feliu, *ACS Catal.*, **2**, 901 (2012).

44. T. Biegler, D. Rand, and R. Woods, *J. Electroanal. Chem. Interfacial Electrochem.*, **29**, 269 (1971).
45. M. K. Bates, Q. Jia, N. Ramaswamy, R. J. Allen, and S. Mukerjee, *The journal of physical chemistry. C, Nanomaterials and interfaces*, **119**, 5467 (2015).
46. H. Wang and H. c. D. Abruña, *J. Am. Chem. Soc.*, **139**, 6807 (2017).
47. K. Elbert, J. Hu, Z. Ma, Y. Zhang, G. Chen, W. An, P. Liu, H. S. Isaacs, R. R. Adzic, and J. X. Wang, *ACS Catal.*, **5**, 6764 (2015).
48. S. M. Alia and Y. Yan, *J. Electrochem. Soc.*, **162**, F849 (2015).
49. J. Zheng, W. Sheng, Z. Zhuang, B. Xu, and Y. Yan, *Science advances*, **2**, e1501602 (2016).
50. E. G. Mahoney, W. Sheng, Y. Yan, and J. G. Chen, *ChemElectroChem*, **1**, 2058 (2014).
51. Z. Cao, Q. Chen, J. Zhang, H. Li, Y. Jiang, S. Shen, G. Fu, B.-A. Lu, Z. Xie, and L. Zheng, *Nature communications*, **8**, 15131 (2017).
52. M. E. Scofield, Y. Zhou, S. Yue, L. Wang, D. Su, X. Tong, M. B. Vukmirovic, R. R. Adzic, and S. S. Wong, *ACS Catal.*, **6**, 3895 (2016).
53. J. Ohyama, D. Kumada, and A. Satsuma, *Journal of Materials Chemistry A*, **4**, 15980 (2016).
54. R. Subbaraman, D. Tripkovic, D. Strmcnik, K.-C. Chang, M. Uchimura, A. P. Paulikas, V. Stamenkovic, and N. M. Markovic, *Science*, **334**, 1256 (2011).
55. M. Gong, W. Zhou, M.-C. Tsai, J. Zhou, M. Guan, M.-C. Lin, B. Zhang, Y. Hu, D.-Y. Wang, and J. Yang, *Nature communications*, **5**, 4695 (2014).
56. N. Ramaswamy, S. Ghoshal, M. K. Bates, Q. Jia, J. Li, and S. Mukerjee, *Nano Energy*, **41**, 765 (2017).
57. H. Yin, S. Zhao, K. Zhao, A. Muqsit, H. Tang, L. Chang, H. Zhao, Y. Gao, and Z. Tang, *Nature communications*, **6**, 6430 (2015).
58. J. Ohyama, T. Sato, Y. Yamamoto, S. Arai, and A. Satsuma, *J. Am. Chem. Soc.*, **135**, 8016 (2013).
59. M. K. Bates, Q. Jia, N. Ramaswamy, R. J. Allen, and S. Mukerjee, *J. Phys. Chem. C*, **119**, 5467 (2015).
60. J. Li, S. Ghoshal, M. K. Bates, T. E. Miller, V. Davies, E. Stavitski, K. Attenkofer, S. Mukerjee, Z. F. Ma, and Q. Jia, *Angew. Chem., Int. Ed.*, **56**, 15594 (2017).
61. A. Serov, *Development of PGM-free Catalysts for Hydrogen Oxidation Reaction in Alkaline Media*, in, U. S. Department of Energy Editor, https://www.hydrogen.energy.gov/pdfs/review16/fc130_serov_2016_o.pdf (2016).
62. T. Sun, C. Zhang, J. Chen, Y. Yan, A. A. Zakhidov, R. H. Baughman, and L. Xu, *Journal of Materials Chemistry A*, **3** (2015).
63. J. Lu, L. Zhang, S. Jing, L. Luo, and S. Yin, *Int. J. Hydrogen Energy*, **42**, 5993 (2017).
64. Y. Zheng, Y. Jiao, Y. Zhu, L. H. Li, Y. Han, Y. Chen, M. Jaroniec, and S.-Z. Qiao, *J. Am. Chem. Soc.*, **138**, 16174 (2016).
65. X. Zou, X. Huang, A. Goswami, R. Silva, B. R. Sathe, E. Mikmeková, and T. Asefa, *Angew. Chem.*, **126**, 4461 (2014).
66. D. Strmcnik, M. Uchimura, C. Wang, R. Subbaraman, N. Danilovic, V. van der, A. P. Paulikas, V. R. Stamenkovic, and N. M. Markovic, *Nat Chem*, **5**, 300 (2013).
67. N. Danilovic, R. Subbaraman, D. Strmcnik, K. C. Chang, A. Paulikas, V. Stamenkovic, and N. M. Markovic, *Angew. Chem.*, **124**, 12663 (2012).
68. P. Rheinländer, S. Henning, J. Herranz, and H. A. Gasteiger, *ECS Trans.*, **50**, 2163 (2013).
69. W. Sheng, Z. Zhuang, M. Gao, J. Zheng, J. G. Chen, and Y. Yan, *Nature communications*, **6**, 5848 (2015).
70. D. Strmcnik, M. Uchimura, C. Wang, R. Subbaraman, N. Danilovic, D. Van Der Vliet, A. P. Paulikas, V. R. Stamenkovic, and N. M. Markovic, *Nature chemistry*, **5**, 300 (2013).
71. D. Santos, C. Sequeira, D. Macciò, A. Saccone, and J. Figueiredo, *Int. J. Hydrogen Energy*, **38**, 3137 (2013).
72. J. Zheng, S. Zhou, S. Gu, B. Xu, and Y. Yan, *J. Electrochem. Soc.*, **163**, F499 (2016).
73. R. K. Shervedani and A. R. Madram, *Electrochim. Acta*, **53**, 426 (2007).
74. S. i. Tanaka, N. Hirose, T. Tanaki, and Y. H. Ogata, *J. Electrochem. Soc.*, **147**, 2242 (2000).
75. J. Weininger and M. Breiter, *J. Electrochem. Soc.*, **111**, 707 (1964).
76. R. Bocutti, M. Saeki, A. Florentino, C. Oliveira, and A. Angelo, *Int. J. Hydrogen Energy*, **25**, 1051 (2000).
77. H. Dong, T. Lei, Y. He, N. Xu, B. Huang, and C. Liu, *Int. J. Hydrogen Energy*, **36**, 12112 (2011).
78. A. G. Oshchepkov, A. Bonnefont, V. A. Saveleva, V. Papaefthimiou, S. Zafeiratos, S. N. Pronkin, V. N. Parmon, and E. R. Savinova, *Top. Catal.*, **59**, 1319 (2016).
79. R. K. Shervedani, A. H. Alinoori, and A. R. Madram, *J New Mater Electrochem Syst*, **11**, 259 (2008).
80. J. Kubisztal, A. Budniok, and A. Lasia, *Int. J. Hydrogen Energy*, **32**, 1211 (2007).
81. Z. Zheng, N. Li, C.-Q. Wang, D.-Y. Li, Y.-M. Zhu, and G. Wu, *Int. J. Hydrogen Energy*, **37**, 13921 (2012).
82. I. Herraiz-Cardona, C. González-Buch, C. Valero-Vidal, E. Ortega, and V. Pérez-Herranz, *J. Power Sources*, **240**, 698 (2013).
83. A. Kellenberger, N. Vaszilcsin, W. Brandl, and N. Duteanu, *Int. J. Hydrogen Energy*, **32**, 3258 (2007).
84. K. Shinozaki, J. W. Zack, R. M. Richards, B. S. Pivovar, and S. S. Kocha, *J. Electrochem. Soc.*, **162**, F1144 (2015).
85. S. Gu, W. Sheng, R. Cai, S. M. Alia, S. Song, K. O. Jensen, and Y. Yan, *Chem. Commun.*, **49**, 131 (2013).
86. K. Tammeveski, T. Tenno, J. Claret, and C. Ferrater, *Electrochim. Acta*, **42**, 893 (1997).
87. N. M. Marković and P. N. Ross Jr, *Surf. Sci. Rep.*, **45**, 117 (2002).
88. N. M. Markovića, S. T. Sarraf, H. A. Gasteiger, and P. N. Ross, *J. Chem. Soc., Faraday Trans.*, **92**, 3719 (1996).